CBX7 is involved in the progression of cervical cancer through the ITGβ3/TGFβ1/AKT pathway

PING TIAN[1,2*], JINGLAN DENG[3*], CAILING MA[1,4*], AINIPA MIERSHALI[5], GULIKEZI MAIMAITIREXIATI[5], QI YAN[5], YATING LIU[3], HATIMIHAN MAIMAITI[5], YUTING LI[5], CHANGHUI ZHOU[5], JINGQIN REN[5], LU DING[6,7] and RONG LI[1,5]

[1]State Key Laboratory of Pathogenesis, Prevention and Treatment of High Incidence Diseases in Central Asia, Xinjiang Medical University, Urumqi, Xinjiang Uyghur Autonomous Region 830054; [2]Department of Nosocomial Infection Management, The Fifth Affiliated Hospital, Xinjiang Medical University, Urumqi, Xinjiang Uyghur Autonomous Region 830011; [3]College of Nursing, Xinjiang Medical University, Urumqi, Xinjiang Uyghur Autonomous Region 830054; [4]Department of Gynecology, Xinjiang Medical University Affiliated First Hospital, Urumqi, Xinjiang Uyghur Autonomous Region 830011; [5]Department of Child, Adolescent and Maternal Hygiene, College of Public Health, Xinjiang Medical University; [6]Postdoctoral Research Center on Public Health and Preventive Medicine, Xinjiang Medical University, Urumqi, Xinjiang Uyghur Autonomous Region 830054; [7]Department of Orthopaedics, Xinjiang Medical University Affiliated Traditional Chinese Medicine Hospital, Urumqi, Xinjiang Uyghur Autonomous Region 830000, P.R. China

Received May 22, 2023; Accepted October 2, 2023

DOI: 10.3892/ol.2023.14147

Abstract. The chromobox protein homolog 7 (CBX7) serves a tumor-suppressive role in human malignant neoplasias. The downregulation of CBX7 is associated with the poor prognosis and aggressiveness of various human cancers. However, the biological functions and underlying mechanisms of CBX7 in cervical cancer remain unclear. The present study investigated the role and mechanism of CBX7 in cervical cancer. Lentivirus and siRNA were used to construct cervical cancer cells with stable CBX7 knockdown and SiHa xenograft models. The cell growth, migration, invasion and apoptosis were observed through *in vivo* and *in vitro* experiments. The expression levels of CBX7, integrin β3 (ITGβ3), transforming growth factor β1 (TGFβ1), phosphatidylinositol-3-kinase (PI3K), AKT, E-cadherin (E-cad) and vimentin (VIM) were detected by western blot analysis and reverse transcription-quantitative PCR. The correlation between CBX7 and these genes was analyzed. TGFβ1 was also silenced through shRNA in cells with stable CBX7 knockdown to detect its effect on cell growth, invasion and apoptosis, and on pathway-related gene expression. It was revealed that knockdown of CBX7 promoted the proliferation, migration, and invasion of cervical cancer cells, and inhibited apoptosis. In addition, CBX7 knockdown promoted tumor growth *in vivo*. Correlation analysis demonstrated that CBX7 was negatively correlated with ITGβ3, TGFβ1, PI3K, AKT, phosphorylated AKT and VIM, but positively correlated with E-cad. Moreover, the knockdown of TGFβ1 reversed the promotion of cell proliferation and inhibition of apoptosis induced by CBX7 knockdown and attenuated the increase of ITGβ3, TGFβ1, PI3K, AKT and VIM caused by CBX7 knockdown. In conclusion, the findings of the present study indicated that the downregulation of CBX7 enhances cell migration and invasion while inhibiting cell apoptosis in cervical cancer by modulating the ITGβ3/TGFβ1/AKT signaling pathways.

Correspondence to: Professor Lu Ding, Postdoctoral Research Center on Public Health and Preventive Medicine, Xinjiang Medical University, 393 Xinyi Road, Urumqi, Xinjiang Uyghur Autonomous Region 830054, P.R. China
E-mail: lurong_618@126.com

Professor Rong Li, Department of Child, Adolescent and Maternal Hygiene, College of Public Health, Xinjiang Medical University, 393 Xinyi Road, Urumqi, Xinjiang Uyghur Autonomous Region 830054, P.R. China
E-mail: lirong_xinjiang@126.com

[*]Contributed equally

Abbreviations: CBX7, chromobox homolog 7; E-cad, E-cadherin; HPV, human papillomavirus; ITGβ3, integrin β3; PRC1, polycomb repressive complex 1; TGFβ1, transforming growth factor β1

Key words: cervical cancer, chromobox homolog 7, integrin β3, transforming growth factor β1

Introduction

Cervical cancer is one of the most common gynecological tumors and its incidence ranks fourth worldwide in gynecological tumors (1). Although its mortality rate has been declining in recent years, its morbidity and the number of overall

cancer-related deaths are on the rise. There are still >500,000 new cases and >250,000 cancer-related deaths worldwide each year, and the 5-year survival rate is only 64.2% (2). In addition, given that certain women have exceeded the recommended age for the human papillomavirus (HPV) vaccine, and not all cases of cervical cancer are attributed to HPV infection, certain patients still experience a progressive development into advanced cancer (3). Therefore, it is necessary to further explore the mechanism of cervical cancer and identify novel therapeutic targets.

Chromobox homolog 7 (CBX7) belongs to the polycomb repressive complex 1 (PRC1) family (4). The expression of CBX7 in tumors varies, and it plays several functions in tumor occurrence and development. The level of CBX7 is low in some tumors such as breast cancer, bladder cancer, colon cancer and glioma, indicating that it may be a tumor suppressor gene (5-8). *In vitro* and *in vivo* experiments have revealed that overexpression of CBX7 could inhibit the progression of glioma (9,10). In pancreatic cancer, CBX7 was revealed to negatively regulate the survival, drug resistance and migration of pancreatic cancer cells (11). In lung cancer, CBX7 was demonstrated to enhance the sensitivity of lung cancer cells to chemotherapeutic drugs (12). However, in gastric cancer, lymphoma and prostate, and ovarian cancer CBX7 is an oncogene (13-16). For example, Ni *et al* (13) found that CBX7 overexpression in gastric cancer cells promotes tumor progression. However, the effect of CBX7 on cervical cancer remains unclear.

Gene ontology map of 44 genes revealed 13 physiologically important cellular pathways, such as integrin (ITG), transforming growth factor β1 (TGFβ1), phosphatidylinositol-3-kinase (PI3K), cadherin and other signaling pathways (17). Rapisarda *et al* revealed that downregulation of CBX7 expression promoted the expression of ITG, which further activated TGFβ (18). TGFβ1 can reduce the expression of E-cadherin (E-cad) and induce epithelial-mesenchymal transition (EMT) (19,20). The integrin β3 (ITGβ3)/AKT signaling pathway can promote the growth of platelet-induced hemangioendothelioma (21). Ni *et al* determined that the mechanism of CBX7 underlying its inhibitory effect on cell growth may involve the AKT signaling pathway (11). A previous study by the authors also demonstrated that low CBX7 expression was positively correlated with poor prognosis in patients with cervical cancer (22). By overexpressing CBX7, it was also revealed that CBX7 promoted apoptosis in cervical cancer cells (23).

In the present study, the effects of CBX7 on the metastasis and apoptosis of cervical cancer cells as well as the underlying mechanisms were further studied.

Materials and methods

Subjects and human cervical cancer samples. A total of 120 patients with cervical cancer admitted to the First Affiliated Hospital of Xinjiang Medical University (Urumqi, China) from January 2018 to Dec 2019 were enrolled in the present study. The patients were aged from 28 to 72 years (mean, 56.88±0.92 years). All patients were diagnosed using histolopathological examination of tissue samples by experts in gynecological pathology. The tumor samples were obtained during high resolution digital colposcopy, cervical colonization and hysterectomy. The matching adjacent non-tumorous tissues were collected and used as controls. Prior written and informed consent was obtained from every patient and the study was approved (approval no. 20120220-01) by the Ethics Review Board of Xinjiang Medical University (Urumqi, China).

Immunohistochemistry. The expression levels of CBX7, ITGβ3, TGFβ1, PI3K, AKT, phosphorylated (p)-AKT, vimentin (VIM) and E-cad in the tissue were determined by immunohistochemistry, using a rabbit polymer method detection system (cat. no. PV6001; OriGene Technologies, Inc.). The tissue samples were fixed with 4% paraformaldehyde for 24 h at room temperature, dehydrated with graded alcohol series, embedded in paraffin, and cut into 4-μm serial sections. Tissue slides (4 μm) were then deparaffinized at 60˚C, followed by treatment with 100% xylene for 20 min and rehydration in graded series of ethanol at room temperature. Followingly, the sections were incubated in 3% H_2O_2 (cat. no. 1301; Dezhou Dexinkang Disinfection Products Co., Ltd.) at room temperature for 20 min. The antigen retrieval was performed with 0.01 M citrate buffer at 95˚C for 10 min. After blocking with normal sheep serum (1:100; cat. no. SAP-9100; OriGene Technologies, Inc.) at room temperature for 30 min, the section was incubated with anti-CBX7 (1:200; cat. no. ab21873; Abcam), anti-ITGβ3 (1:500; cat. no. ab7166; Abcam), anti-TGFβ1 (1:200; cat. no. BA0290; Boster Biological Technology; https://www.boster.com.cn/index/products/productslist?catid=all&keywords=BA0290), anti-PI3K (1:100; cat. no. E-AB-22165; Elabscience Biotechnology, Inc.), anti-AKT (1:1,000; cat. no. ab8805; Abcam), p-AKT (1:100; cat. no. 4060; CST Biological Reagents Co., Ltd.), anti-E-cad (1:500; cat. no. ab40772; Abcam) and anti-VIM (1:300; cat. no. ab92547; Abcam) monoclonal antibodies, respectively, at 4˚C overnight. The section was then incubated with HRP-conjugated anti-rabbit En Vision system (1:200; cat. no. PV-6001; OriGene Technologies, Inc.) at 37˚C for 20 min, followed by staining for 3-5 min with diaminobenzidine tetrahydrochloride (cat. no. ZLI-9018; OriGene Technologies, Inc.). The sections were then counterstained with hematoxylin for 20 s at room temperature. Finally, the sections were observed under an IX71 inverted light microscope (Magnificantion: 200x; Olympus, Tokyo, Japan). Immunohistochemistry was assessed using a semiquantitative approach, whereby the intensity of staining and the percentage of positive cells were combined. The staining intensity was categorized as absent (0 points), weak (1 point), moderate (2 points) or strong (3 points). The mean percentage of positively stained cells was scored as follows: i) 0 points (<25%), ii) 1 point (25-50%), iii) 2 points (51-75%) and iv) 3 points (76-100%). The total score was calculated by multiplying the staining intensity and the percentage of positive cells, ranging from 0 to 9. The scores ≤1 were classified as negative expression, while scores >1 were classified as positive expression.

Cell lines. HeLa (cat. no. ZQ0068) and SiHa (cat. no. ZQ0129) cells were purchased from Shanghai Zhong Qiao Xin Zhou Biotechnology Co., Ltd. These cell lines were incubated in DMEM (cat. no. 11965-092; Gibco; Thermo Fisher Scientific, Inc.) supplemented with 10% fetal bovine serum (cat. no. 10091-148; Gibco; Thermo Fisher Scientific, Inc.),

100 U/ml penicillin and 100 μg/ml of streptomycin (30-002-CI; Cellgro; Corning, Inc.). The cells were maintained at 37˚C and 95% humidity in a 5% CO_2 atmosphere. Once the cells reached 80-90% confluency, they were subcultured.

Establishment of stable CBX7 knockdown in cervical cancer cells. To stably knockdown CBX7 expression in cervical cancer cells, four CBX7-specific siRNAs were designed and synthesized by Beijing CorreGene Biotechnology Co., Ltd. Briefly, the plasmids, including LentiCRTM-spKO-CBX7-sg1 (10 μg), LentiCRTM-spKO-CBX7-sg2 (10 μg), LentiCRTM-spKO-CBX7-sg3 (10 μg), LentiCRTM-spKO-CBX7-sg4 (10 μg), and LentiCRISPR E (10 μg), as well as the auxiliary plasmids including psPAX2 (10 μg) and pVSVG (5 μg) were packaged into lentiviruses and co-transfected into 293T cells using Lipofiter^{TM} (Invitrogen; 11668-019). The culture medium was changed after 18 h. The transfection was performed for 48 h. On days 3, 4 and 5, the lentiviruses were collected and centrifuged at 4˚C, 2,000 x g for 10 min. After removing cell debris, the supernatant was collected and centrifuged at 4˚C, 9,000 x g for 120 min. Next, low-passage SiHa and HeLa cells were seeded in 10-cm culture dishes and infected with LentiCRTM-spKO-CBX7-sg1, LentiCRTM-spKO-CBX7-sg2, LentiCRTM-spKO-CBX7-sg3, LentiCRTM-spKO-CBX7-sg4 and LentiCRISPR E viruses for 24 h at 37˚C and 5% CO_2 at a multiplicity of infection of 30. The control cells were not infected. The cells were then incubated overnight at 37˚C and 5% CO_2. At 24-48 h after infection, cells were cultured in the medium containing 1 μg/ml of puromycin. Every day, the DMEM containing 1 μg/ml puromycin was replaced. After 7 days, the resistant cells were collected and seeded into 25 cm^2 culture flasks for further cultivation. The transduction efficiency was confirmed using 24 h after transduction. The method of constructing HeLa cell CBX7 gene-knockout cell lines is the same as that for SiHa cells. The knockdown efficiency of CBX7-shRNA lentivirus was determined using western blot analysis. LentiCRTM-spKO-CBX7-sg1 (GGAGCCAGA AGAGCA CATCT) and LentiCRTM-spKO-CBX7-sg4 (gcTGCCGA GTGGGCACGTCA) were selected as the lentiviruses with the optimal knockdown efficiency for HeLa and SiHa, respectively. HeLa and SiHa cells were divided into 3 groups: the SiCBX7 group (transfected with LentiCRTM-spKO-CBX7-sg), the SiCBX7-EVC group (transfected with LentiCRISPR E), and the control (CTRL) group (non-transfected cells).

Knockdown of TGFβ. TGFβ-specific shRNAs (TGFβ1-HOMO-875, TGFβ1-HOMO-1158, and TGFβ1-HOMO-1408) and control shRNA were designed and synthesized by Beijing Kerui Biotechnology Co., Ltd. shRNA sequences used for the knockdown of TGFβ : TGFβ1-HOMO-875 forward, 5'-GCU ACCGCUGCUGUGGCUATT-3' and reverse, 5'-UAGCCA CAGCAGCGGUAGCTT-3'; TGFβ1-HOMO-1158 forward, 5'-GAGGUCACCCGCGUGCUAATT' and reverse, 5'-UUA GCACGCGGGUGACCUCTT-3' and TGFβ1-HOMO-1408 forward, 5'-GCGACUCGCCAGAGUGGUUTT' and reverse, 5'-AACCACUCUGGCGAGUCGCTT-3'. The sequence of control shRNA was forward, 5'-UUCUCCGAACGUGUCACG UTT-3 and reverse, 5'ACGUGACACGUUCGGAGAATT-3. The transfection of control shRNA or TGFβ shRNAs into SiHa and HeLa cells was carried out using Lipofectamine 2000 transfection reagent (cat. no. 11668-019; Invitrogen; Thermo Fisher Scientific, Inc.) at room temperature. Briefly, cells in the logarithmic phase of growth and in good condition were used. The shRNAs (4 μg) and Lipofectamine 2000 (5 μl) were separately diluted in a 100 μl serum-free medium and incubated at room temperature for 20 min. They were then mixed and incubated with cells at 37˚C and 5% CO_2. After incubation for 5 h, the culture medium was replaced with a complete medium containing 10% fetal bovine serum, and the cells were further cultured for 48 h. The RT-qPCR determined the TGFβ shRNA with the optimal knockdown efficiency (24). The cells were divided into 6 groups: siCBX7 + NC, siCBX7-EVC + NC, CTRL + NC group, siCBX7 + shRNATGFβ1, siCBX7-EVC + shRNATGFβ1 and CTRL+ shRNATGFβ1 group.

MTT viability assay. HeLa and SiHa cells with knockdown of CBX7 or TGFβ1 ($1.0x10^4$ cells/well) were plated in 96 well plates. At the following timepoints: 0, 12, 24, 48, 72 and 96 h, 20 μl of MTT (cat. no. BS186; Biosharp Life Sciences) was added and incubated at 37˚C for 4 h. The cells were then treated with 150 μl of DMSO (cat no. D8370; Beijing Solarbio Science & Technology Co., Ltd.) for 10 min under agitation in a light-protected environment. The absorbance was subsequently measured at 570 nm using a microplate reader from Thermo Fisher Scientific, Inc.

Wound healing assay. HeLa and SiHa cells with stable knockdown of CBX7 or TGFβ1 ($5x10^5$ cells/well) were seeded in six-well plates and placed in a 37˚C cell culture incubator. The cells were cultured until cell confluence reached >90%. A wound was then created vertically using a 1-ml pipette tip. After washing with PBS, cells were incubated with fresh DMEM without FBS. The wound was photographed at 0, 24 and 48 h of culture using an IX71 inverted light microscope (magnification, x100x, Olympus Corporation). The distance of the wound was measuredusing Image J software (version 1.50; National Institutes of Health), and the results were expressed as the percentage of the remaining wound area. This assay was performed in triplicate.

Cell migration assay. Cell migration ability was analyzed using a Transwell chamber (cat. no. 353097; Corning, Inc.). After serum-starved culture overnight, a total of $1x10^4$ HeLa and SiHa cells with stable knockdown of CBX7 or TGFβ1 were plated in the upper chambers of Transwell plates in 100 μl of serum-free medium. The lower chamber was filled with a medium containing 10% fetal bovine serum, which served as the chemoattractant. Following incubation at 37˚C for 24 h, cells that did not migrate through the pores were carefully wiped out with cotton wool. The migratory cells were fixed with pure methanol for 30 min, stained with 0.1% crystal violet for 20 min at room temperature, and observed with an IX71 inverted light microscope (Olympus Corporation).

Cell apoptotic analysis by flow cytometry. Cell apoptotic analysis was performed using an Annexin-V/PI assay kit (cat. no. KGA1026; Nanjing KeyGen Biotech Co., Ltd.). Briefly, HeLa and SiHa cells ($1x10^{*6}$/ml) with stable knockdown of CBX7 or TGFβ1 were cultured for 24 h, the cells

Table I. Primer sequences of reverse transcription-quantitative PCR.

Gene	Primer	Sequence	Size
Homo β-actin	Forward	5'-AGCGAGCATCCCCCAAAGTT-3'	285 bp
	Reverse	5'-GGGCACGAAGGCTCATCATT-3'	
Homo TGFβ1	Forward	5'-CAGCAACAATTCCTGGCGATACCT-3'	140 bp
	Reverse	5'-CGCTAAGGCGAAAGCCCTCAAT-3'	
Homo ITGβ3	Forward	5'-TGGGGCTGATGACTGAGAAG-3'	206 bp
	Reverse	5'-ACGCACTTCCAGCTCTACTT-3'	
Homo AKT	Forward	5'-ACACCAGGTATTTTGATGAGGA-3'	143 bp
	Reverse	5'-TCAGGCCGTGCCGCTGGCCGAGTAG-3'	
Homo VIM	Forward	5'-TGAGTACCGGAGACAGGTGCAG-3'	119 bp
	Reverse	5'-TAGCAGCTTCAACGGCAAAGTTC-3'	
Homo CBX7	Forward	5'-CGGAAGAAGCGCGTGCGGAAGGGT-3'	372 bp
	Reverse	5'-GCGGAGCGGGAAGGGCAGGGTGGG-3'	
Homo PI3K	Forward	5'-GACTCAAAAAGGTGTTCGG-3'	311 bp
	Reverse	5'-ACAAGTTATAGGGCTCGGC-3'	
Homo E-cad	Forward	5'-ACGCATTGCCACATACACT-3'	149 bp
	Reverse	5'-CCATGACAGACCCCTTAAA-3'	

TGFβ1, transforming growth factor β1; ITGβ3, integrin β3; VIM, vimentin; CBX7, chromobox protein homolog 7; PI3K, phosphatidylinositol-3-kinase; E-cad, E-cadherin; bp, base pairs.

were collected and washed. Next, the cells were stained with Annexin-V-FITC/PI at room temperature in the dark for 10~15 min. Finally, the samples were analyzed on a Cyto FLEX flow cytometer (Beckman Coulter, Inc.). The data were analyzed using FlowJo v10 (FlowJo LLC).

Animals. Female BALB/c nude mice (age, 4-6 weeks old, weighing 18±2g, n=36) were obtained from Beijing Vital River Laboratory Animal Technology Co., Ltd. They were housed under strict pathogen-free conditions with a temperature of 20-24˚C, a relative humidity of 50%, and a 12-h light-dark cycle. All mice were provided food and water ad libitum. All animal experiment procedures were approved (approval no. 20120220-01) by the Ethics Committee of Xinjiang Medical University.

Xenograft tumor model. SiHa control cells and SiHa cells with stable transfection of siCBX7-EVC and siCBX7 ($5x10^6$ cells in 100 μl PBS) were injected subcutaneously into the right flank of each nude mouse (7 weeks old, n=12/group). The tumors were measured every three days using a vernier caliper and the volumes of tumors were calculated using the following formula: Volume (mm^3)=length x $width^2$ x 0.5. After 30 days of tumor formation, tumor measurements were conducted every three days. On day 45 post-inoculation, the mice were euthanized by intraperitoneal injection of 60 mg/kg pentobarbital, followed by rapid cervical dislocation. To confirm death, the absence of breathing and nerve reflexes were used as criteria. The tumors were dissected and examined using a stereoscopic microscope.

Western blotting. Total protein was were extracted from HeLa and SiHa cells (with stable knockdown of CBX7 or TGFβ1 knockdown) and tumor tissues using RIPA lysis buffer (cat. no. 20188; Sigma-Aldrich; Merck KGaA). The protein concentration was determined using a BCA Protein Assay kit. Proteins (50 μg/lane) were then subjected to 10% SDS-PAGE electrophoresis and PVDF membrane transfer. The membranes were blocked with 5% skimmed milk and 0.1% Tween-20 in Tris-buffered saline for 2 h at room temperature. After blocking, the membrane was incubated with the corresponding primary antibodies at 4˚C overnight. The primary antibodies included anti-TGFβ1 (1:300; BA0290; Boster Biological Technology), anti-CBX7 (1:500 dilution; cat. no. ab21837; Abcam), anti-vimentin (1:2,000; cat. no. 10366-1-AP; Proteintech Group, Inc.), anti-p-AKT (1:2,000; cat. no. 4060; CST Biological Reagents Co., Ltd.), anti-PI3K p85 (1:2,000; cat. no. bs-3332R; BIOSS), anti-AKT1 (1:1,000; cat. no. ab8805; Abcam), anti-ITGβ3 (1:1,000; cat. no. ab7166; Abcam), anti-E-cad (1:1,000; cat. no. ab40772; Abcam) and anti-β-actin (1:500; cat. no. BM0627; Boster Biological Technology). Finally, the membranes were incubated with horseradish peroxidase-conjugated secondary antibody (1:10,000; cat. no. BA1054; Boster Biological Technology) for 2 h at room temperature. The signal was visualized using ECL western blotting detection reagent (cat. no. PE0010; Beijing Solarbio Science & Technology Co., Ltd.). The blots were analyzed with a gel imaging analysis system (Bio-Rad Laboratories, Inc.). Relative protein expresion levels were quantified using Quantity One 1-D software (version 4.62; Bio-Rad Laboratories, Inc.).

RT-qPCR. Total RNA was extracted from cells and tumor tissues using Trizol® reagent (Invitrogen; Thermo Fisher Scientific, Inc.) and then reverse transcribed into cDNA using

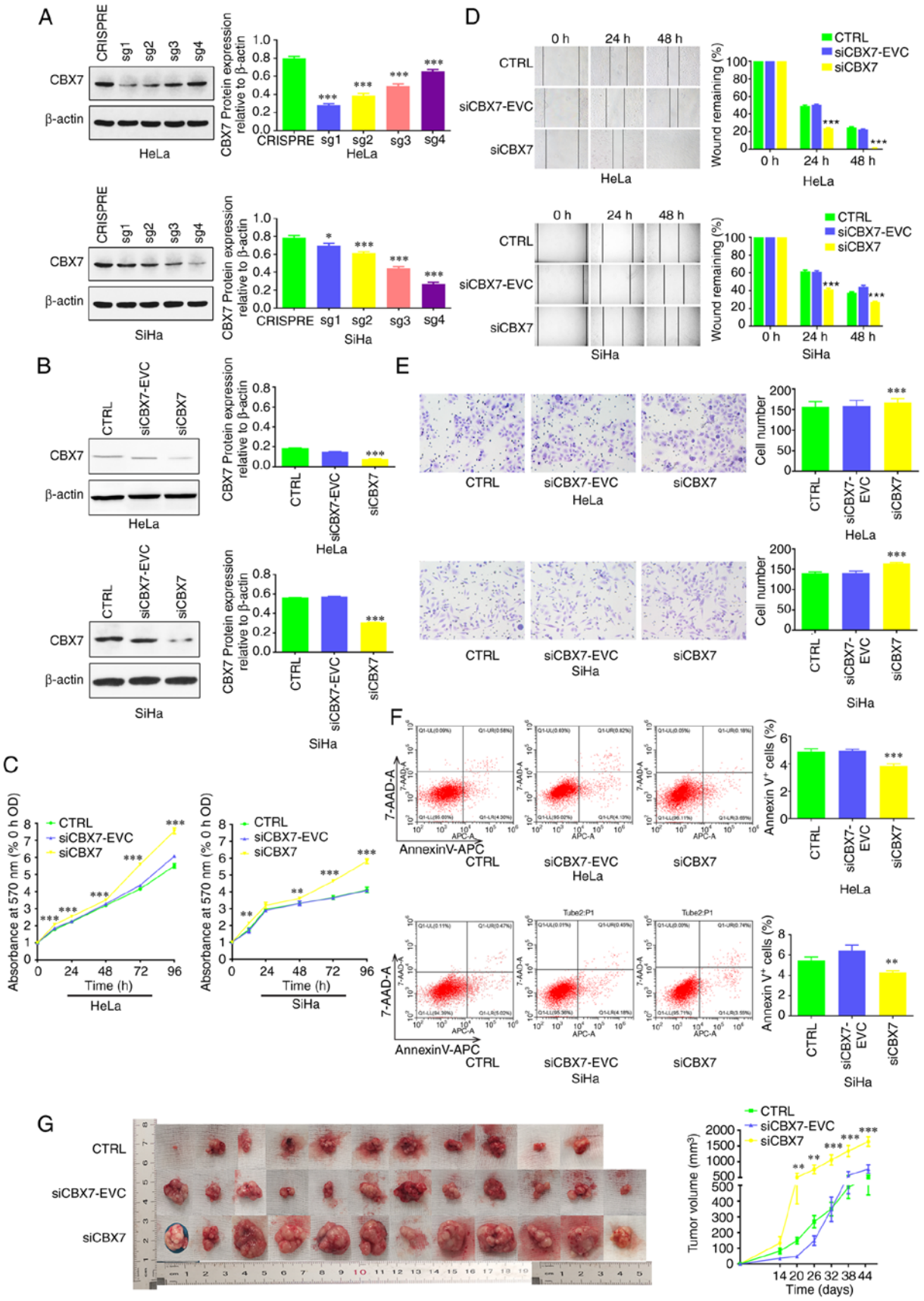

Figure 1. Low expression of CBX7 promotes the growth, migration, invasion and apoptosis inhibition of cervical cancer cells. (A) Expression of CBX7 in cervical cancer cells with stable knockdown of CBX7 was verified by western blotting. (B) The expression of CBX7 in stalby transfected cervical cancer cells was verified by western blotting. (C) The effect of CBX7 on the proliferation of HeLa and SiHa cells was detected by MTT assay. (D) The effect of CBX7 on the migration of HeLa and SiHa cells was detected by wound healing assay (Magnification: 100x). (E) The effect of CBX7 on the invasion of HeLa and SiHa cells was detected by Transwell assay (Magnification: 200x). (F) The effect of CBX7 on the apoptosis of cervical cancer cells was detected by flow cytometry. (G) The effect of CBX7 on the growth of cervical carcinoma-transplanted tumors in nude mice. Error bars in all panels represent the mean ± SD. *P<0.05, **P<0.01 and ***P<0.001 compared with the control and siCBX7-EVC. CBX7, chromobox protein homolog 7; CTRL, control; OD, optical density.

Table II. Expression of CBX7, ITGβ3, TGFβ1, PI3K, AKT, p-AKT, E-cad and VIM in cervical cancer and adjacent non-tumorous cervical tissues (N, %).

	CBX7		ITGβ3		TGFβ1		PI3K	
Groups	Negative	Positive	Negative	Positive	Negative	Positive	Negative	Positive
Cervical cancer tissue	71 (59.2)	49 (40.8)	51 (42.5)	69 (57.5)	18 (15.0)	102 (85.0)	29 (24.2)	91 (75.8)
Adjacent non-tumorous cervical tissues	51 (42.5)	69 (57.5)	97 (80.8)	23 (19.2)	60 (50.0)	60 (50.0)	66 (55.0)	54 (45.0)
χ^2	6.018		37.297		33.504		23.852	
P-value	0.014		<0.001		<0.001		<0.001	

	AKT		p-AKT		E-cad		VIM	
Groups	Negative	Positive	Negative	Positive	Negative	Positive	Negative	Positive
CC	59 (49.2)	61 (50.8)	56 (46.7)	64 (53.3)	89 (74.2)	31 (25.8)	27 (22.5)	93 (77.5)
CTRL	87 (72.5)	33 (27.5)	66 (60)	44 (40)	8 (6.2)	122 (93.8)	102 (85.0)	18 (15.0)
χ^2	13.71		4.096		118.710		101.950	
P-value	<0.001		0.043		<0.001		<0.001	

CBX7, chromobox protein homolog 7; ITGβ3, integrin β3; TGFβ1, transforming growth factor β1; p-, phosphorylated; E-cad, E-cadherin; VIM, vimentin; CC, cervical cancer; CTRL, control.

a High Capacity cDNA Reverse Transcription kit (Thermo Fisher Scientific, Inc.). The reaction was conducted at 42˚C for 18 min and 98˚C for 5 min. The levels of mRNA were examined using the SYBR Green Master Mix kit (Invitrogen; Thermo Fisher Scientific, Inc.). The primer sequences are presented in Table I. The thermocycling conditions were as follows: Initial denaturation at 50˚C for 2 min, 95˚C for 10 min, 95˚C for 30 sec and 60˚C for 30 sec for 40 cycles. The internal control was β-actin. The relative mRNA level was calculated with the $2^{\Delta\Delta Cq}$ method (24).

Statistical analysis. All statistical analysis was performed using SPSS 21.0 software (IBM Corp.) and GraphPad software (v.7.0; GraphPad Software; Dotmatics). Data are presented as the mean ± SD of three independent experiments. The differences in the ITGβ3, TGFβ1, PI3K, AKT, p-AKT, VIM and E-cad expression levels between the cervical cancer tissues and adjacent non-tumorous cervical tissues were analyzed by the χ^2 test. The correlation of contingency paired data of CBX7 with other indexes was analyzed by φ) coefficient analysis. One-way ANOVA followed by Tukey's post hoc test or χ^2 method were used for multiple groups or pairwise comparison of multiple groups. P<0.05 was considered to indicate a statistically significant difference.

Results

CBX7 knockdown promotes the proliferation and metastasis but inhibits the apoptosis of cervical cancer cells. CBX7 was first knocked down in cervical cancer cell lines. The results demonstrated that clones of HeLa-CBX7sg1 and SiHa-CBX7sg4 had the lowest CBX7 expression (Fig. 1A). These clones were used in the subsequent experiments. CBX7 expression in these clones was further verified by western blot analysis, which revealed that CBX7 was successfully knocked down (Fig. 1B). Subsequently, to determine the effects of CBX7 on cell proliferation, an MTT assay was performed. The results showed that the OD_{570} of the siCBX7 group significantly increased compared with that of the siCBX7-EVC and CTRL groups, indicating that CBX7 knockdown resulted in significantly increased proliferation (P<0.05; Fig. 1C). The wound healing assay revealed that the wound area of the siCBX7 group was significantly smaller than the other two groups at 48 h, indicating that downregulation of CBX7 significantly promoted cell migration (P<0.05; Fig. 1D). Next, a Transwell assay was performed and revealed that cell migration was also significantly increased by CBX7 knockdown. There was a significant increase in the number of migrated cells in the siCBX7 group (P<0.001; Fig. 1E). Furthermore, flow cytometry revealed that the proportion of apoptotic cells in the siCBX7 group was significantly lower than that in the siCBX7-EVC and CTRL groups (P<0.05; Fig. 1F). Additionally, a xenograft tumor model was subsequently established by injecting infected siCBX7 SiHa cells into nude mice to investigate whether knockdown of CBX7 exerts similar growth-promoting effects *in vivo*. As revealed in Fig. 1G, one nude mouse in the control group did not develop tumors, while the tumor incidence rate for the other two groups was 100%. The largest tumor was observed in the siCBX7 group, with a tumor volume of 1,812.54 mm^3. Statistically, the tumor volume was increased in the siCBX7 group compared with that in the siCBX7-EVC and CTRL (P<0.05; Fig. 1G), demonstrating that

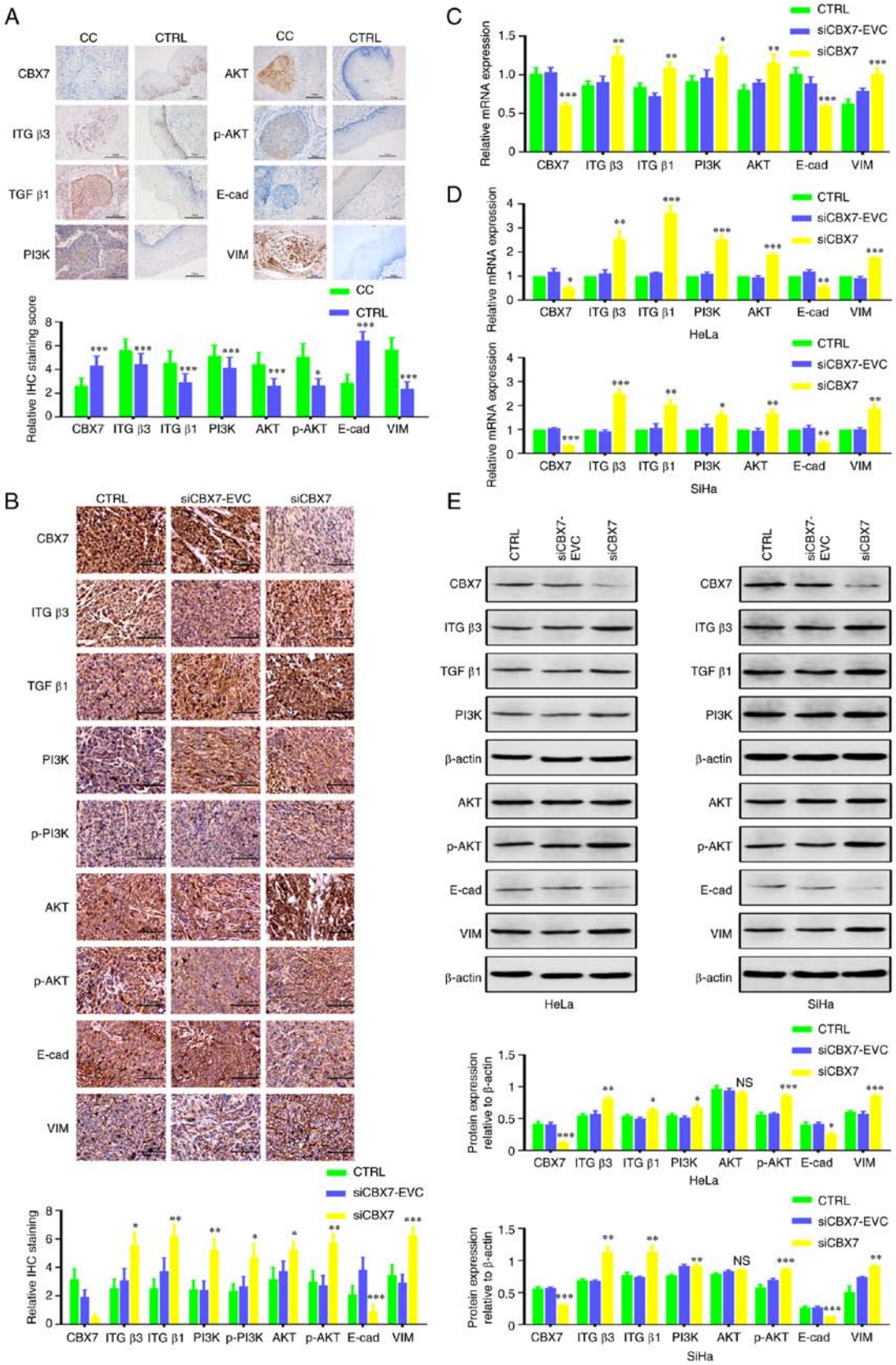

Figure 2. Effect of CBX7 on the expression of ITGβ3, TGFβ1, PI3K, AKT, p-AKT, VIM, and E-cad. (A) Representative images and statistical analysis of IHC detection of CBX7, ITGβ3, TGFβ1, PI3K, AKT, p-AKT, E-cad and VIM protein expression in CC and CTRL tissues (magnificantion: 200x). (B) Representative images and statistical analysis of IHC detection of CBX7, ITGβ3, TGFβ1, PI3K, AKT, p-AKT, E-cad and VIM protein in transplanted tumor tissues (Magnificantion: 200x). (C) The effect of CBX7 on *CBX7, ITGβ3, TGFβ1, PI3K, AKT, p-AKT, E-cad* and *VIM* mRNA in nude mouse-transplanted tumor tissues by reverse transcription-quantitative PCR. (D) The effect of CBX7 on *CBX7, ITGβ3, TGFβ1, PI3K, AKT, p-AKT, E-cad* and *VIM* mRNA in HeLa and SiHa cells. (E) Expression of CBX7, ITGβ3, TGFβ1, PI3K, AKT, p-AKT, E-cad and VIM protein in HeLa and SiHa cells. Error bars in all panels represent the mean ± SD. *P<0.05, **P<0.01 and ***P<0.001 compared with the control and siCBX7-EVC. CBX7, chromobox protein homolog 7; ITGβ3, integrin β3; TGFβ1, transforming growth factor β1; PI3K, phosphatidylinositol-3-kinase; p-, phosphorylated; VIM, vimentin; E-cad, E-cadherin; CC, cervical cancer; CTRL, control; IHC, immunohistochemistry.

Table III. Correlation of CBX7 with ITGβ3, TGFβ1, PI3K, AKT, p-AKT, E-cad and VIM in cervical cancer tissues (N, %).

	ITGβ3 frequency (%)			TGFβ1 frequency (%)		
CBX7	Negative	Positive	Total	Negative	Positive	Total
Negative	21 (17.5)	50 (41.7)	71	5 (4.2)	66 (55.0)	71
Positive	30 (25.0)	19 (15.8)	49	13 (10.8)	36 (30.0)	49
Total no.	51	69	120	18	102	120
Phi (φ)	-0.315			-0.268		
P-value	0.001			0.003		

	PI3K frequency (%)			AKT frequency (%)			p-AKT frequency (%)		
CBX7	Negative	Positive	Total	Negative	Positive	Total	Negative	Positive	Total
Negative	6 (5.0)	65 (54.2)	71	26 (21.7)	45 (37.5)	71	13 (10.8)	58 (48.3)	71
Positive	23 (19.2)	26 (21.7)	49	33 (27.5)	8 (13.3)	49	43 (35.8)	6 (5.0)	49
Total no.	29	91	120	59	61	120	56	64	120
Phi (φ	-0.442			-0.302				-0.684	
P-value	<0.001			0.001				<0.001	

	E-cad frequency (%)			VIM frequency (%)		
CBX7	Negative	Positive	Total	Negative	Positive	Total
Negative	62 (51.7)	9 (7.5)	71	6 (5.0)	65 (52.4)	71
Positive	27 (22.5)	22 (18.3)	49	21 (17.5)	28 (23.3)	49
Total no.	89	31	120	27	93	120
φ)	0.362			-0.405		
P-value	<0.001			<0.001		

CBX7, chromobox protein homolog 7; ITGβ3, integrin β3; TGFβ1, transforming growth factor β1; p-, phosphorylated; E-cad, E-cadherin; VIM, vimentin.

Table IV. Comparison of positive expression rates of key genes in the ITGβ3/TGFβ1 signaling pathway and EMT markers in three groups of nude mice with xenograft tumors (N, %).

		CBX7		ITGβ3		TGFβ1		PI3K		p-PI3K	
Groups	N	Negative	Positive	Negative	Positive	Negative	Positive	Negative	Positive	Negative	Positive
CTRL	11	4 (36.4)	7 (73.6)	4 (36.4)	7 (73.6)	3 (27.3)	8 (72.7)	4 (36.4)	7 (73.6)	3 (27.3)	8 (72.7)
siCBX7-EVC	12	6 (50.0)	6 (50.0)	5 (28.6)	7 (71.4)	5 (28.6)	7 (71.4)	5 (28.6)	7 (71.4)	5 (41.7)	7 (58.3)
siCBX7	12	11 (91.7)	1 (8.3)	1 (8.3)	11 (91.7)	2 (16.7)	10 (83.3)	2 (16.7)	10 (83.3)	3 (25.0)	9 (75.0)
χ^2		4.216		4.274		1.874		2.038		0.886	
P-value		0.040		0.118		0.392		0.383		0.642	

		AKT		p-AKT		E-cad		VIM	
Groups	N	Negative	Positive	Negative	Positive	Negative	Positive	Negative	Positive
CTRL	11	3 (27.3)	8 (72.7)	4 (36.4)	7 (73.6)	6 (45.5)	6 (54.5)	3 (27.3)	8 (72.7)
siCBX7-EVC	12	3 (25.0)	9 (75.0)	5 (28.6)	7 (71.4)	4 (33.3)	8 (66.7)	4 (33.3)	8 (66.7)
siCBX7	12	1 (8.3)	11 (91.7)	1 (8.3)	11 (91.7)	11 (91.7)	1 (8.3)	0 (0.0)	12 (100.0)
χ^2		1.757		4.274		10.485		6.861	
P-value		0.415		0.118		0.005		0.032	

CBX7, chromobox protein homolog 7; ITGβ3, integrin β3; TGFβ1, transforming growth factor β1; PI3K, phosphatidylinositol-3-kinase; p-, phosphorylated; E-cad, E-cadherin; VIM, vimentin; CTRL, control.

the downregulation of CBX7 may promote xenograft tumor growth in nude mice.

Effect of CBX7 on the expression of key genes in the ITGβ3/TGFβ1 signaling pathway and EMT markers. Immunohistochemistry was performed to detect the protein expression of CBX7, ITGβ3, TGFβ1, PI3K, AKT, p-AKT, VIM and E-cad in cancer tissues from humans and mice. As illustrated in Fig. 2A and Table II, the expression of CBX7 and E-cad in human cervical cancer tissues was significantly lower, whereas the expression of ITGβ3, TGFβ1, PI3K, AKT, p-AKT and VIM was significantly higher than those of adjacent tissues (P<0.05). Correlation analysis demonstrated that CBX7 and E-cad expression were positively correlated (φ=0.362; P<0.001); however, CBX7 was negatively correlated with other proteins (all P<0.05; Table III). In xenograft tumor tissues of mice, knockdown of CBX7 increased the level of VIM and decreased expression of E-cad significantly (Fig. 2B; Table IV; P<0.01). In addition, RT-qPCR revealed that CBX7 knockdown significantly increased *VIM, ITGβ3, TGFβ1, PI3K* and *AKT* mRNA levels, and reduced *E-cad* mRNA expression in xenograft tumor tissues (P<0.05) (Fig. 2C).

Similar results were obtained in stable cells with knockdown of CBX7 (Fig. 2D). In HeLa and SiHa cells after CBX7 knockdown, RT-qPCR results showed that knockdown of CBX7 reduced *E-cad* mRNA (57.0%) and increased the mRNA levels of *VIM* (179.5%), *ITGβ3* (253.3%), *TGFβ1* (364.5%), *PI3K* (251.4%) and *AKT* (191.2%) (Fig. 2D). Similarly, the results of western blotting demonstrated that knocking down CBX7 in HeLa and SiHa cells promoted the expression of VIM, ITGβ3, TGFβ1, PI3K and AKT, and reduced the level of E-cad (Fig. 2E and F).

The aforementioned results indicated that CBX7 may regulate the ITGβ3/TGFβ1/AKT signaling pathway and may be involved in the EMT process.

Knockdown of CBX7 promotes cervical cancer progression through the ITGβ3/TGFβ1/AKT signaling pathway. To verify the mechanism of CBX7 in cervical cancer, TGFβ1 of the TGFβ1 pathway was further knocked down and its effect on the proliferation, metastasis and apoptosis of cervical cancer cells was explored. The expression of *TGFβ1* mRNA after transfection of TGFβ1-HOMO-875, TGFβ1-HOMO-1158 and TGFβ1-HOMO-1408 was 0.51, 0.31 and 0.47, respectively, significantly lower than that in the control group (P<0.001) (Fig. 3A). The TGFβ1-HOMO-1158 fragment had the highest knockdown efficiency and was therefore used in subsequent experiments. TGFβ1 expression in control cells or cells with stable knockdown of CBX7 was further verified by RT-qPCR. The results revealed that TGFβ1 was successfully knocked down in each group (Fig. 3B). The MTT assay and Transwell assay demonstrated that the downregulation of CBX7 increased cell proliferation (Fig. 3C) and migration (Fig. 3D) compared with siCBX7-EVC and CTRL groups. Furthermore, the proliferation and migration ability of cells with knockdown of CBX7 and TGFβ1 decreased and were lower than the cells with CBX7 knockdown only at 12, 24, 48 and 72 h. Flow cytometry revealed that the downregulation of CBX7 decreased apoptosis compared with siCBX7-EVC and CTRL groups. Additionally, the apoptosis ability of cells with knockdown of CBX7 and TGFβ1 increased and was higher than the cells with CBX7 knockdown-only (Fig. 3E). Collectively, TGFβ1 silencing reversed the increase in cell proliferation, and migration and reversed the decrease in apoptosis. The aforementioned results

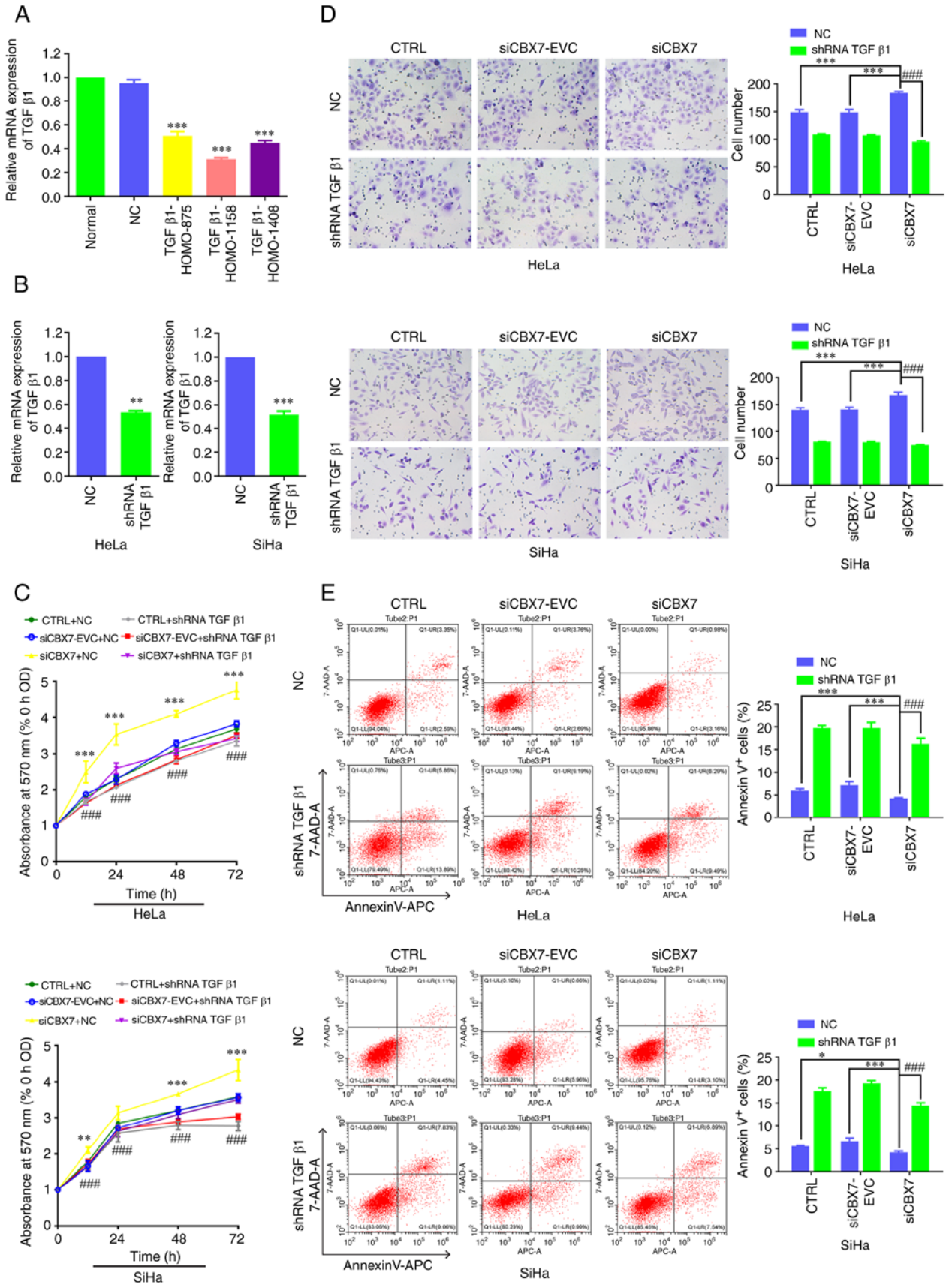

Figure 3. Knockdown of TGFβ1 reverses the effects of CBX7 knockdown on cervical cancer cell proliferation, migration and apoptosis. HeLa and SiHa cells with stable expression of CBX7 knockdown were transfected with TGFβ1 shRNAs. (A) TGFβ1 mRNA was assessed with reverse transcription-quantitative PCR to determine the TGFβ shRNA with the optimal knockdown efficiency. (B) TGFβ1 mRNA expression in each group after transfection with TGFβ1 shRNA. (C) The proliferation ability of HeLa and SiHa cells was detected by MTT assay. (D) The migration ability of HeLa and SiHa cells was analyzed by Transwell assay (Magnificantion: 200x). (E) The apoptosis of HeLa and SiHa cells was assessed using flow cytometry. Error bars in all panels represent the mean ± SD. *P<0.05, **P<0.01 and ***P<0.001, siCBX7 compared with the control and siCBX7-EVC; $^{\#\#\#}$P<0.001, siCBX7 + shRNA TGFβ1 compared with siCBX7. TGFβ1, transforming growth factor β1; CBX7, chromobox protein homolog 7; shRNA, short hairpin RNA; NC, negative control; CTRL, control.

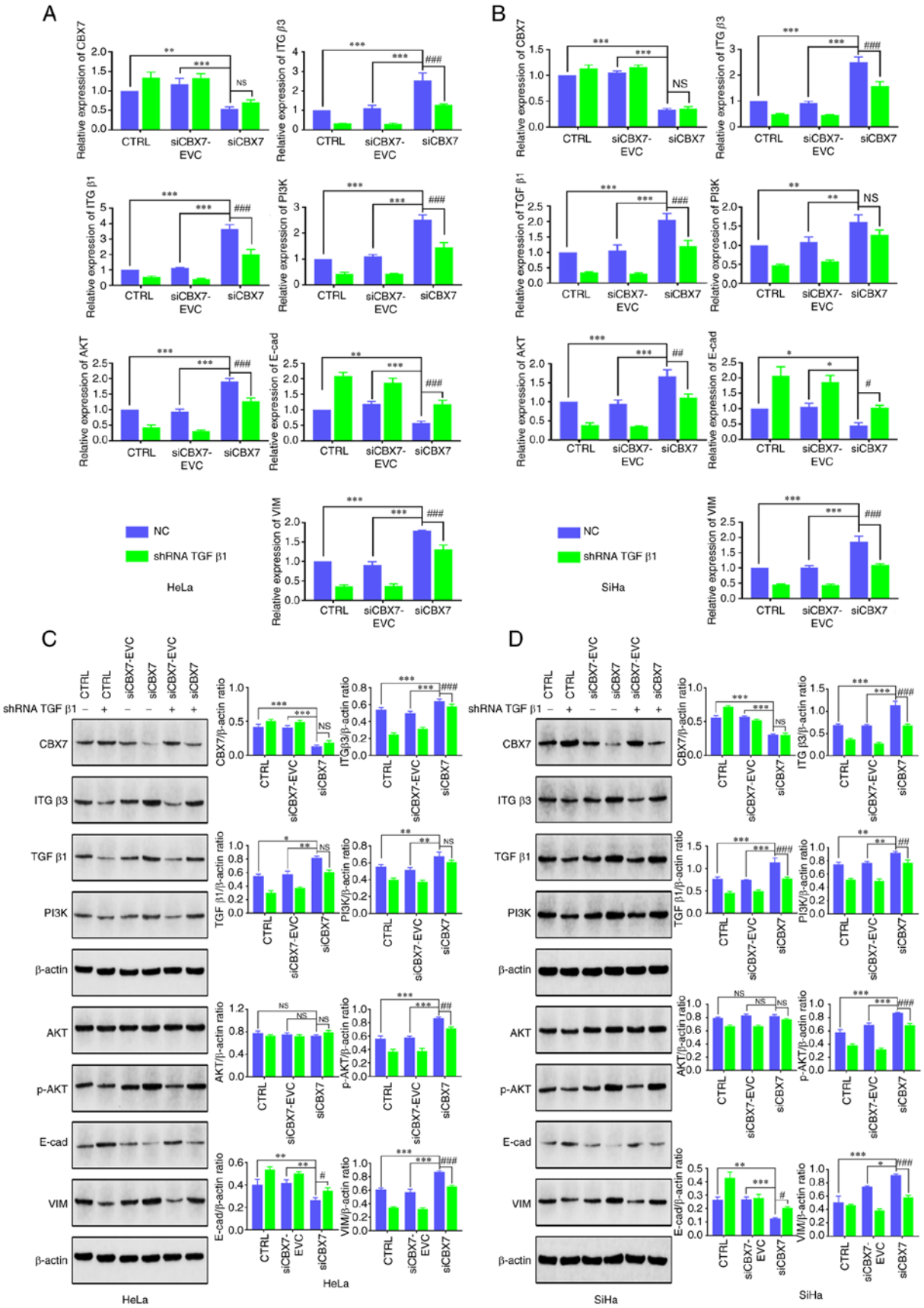

Figure 4. Effect of TGFβ1 silencing and CBX7 knockdown on the expression of key genes in the PI3K/AKT and ITGβ3/TGFβ1 signaling pathways. HeLa and SiHa cells with stable expression of CBX7 knockdown were transfected with silencing plasmids of TGFβ1. The mRNA expression of genes in the PI3K/AKT and ITGβ3/TGFβ1 signaling pathways in (A) HeLa and (B) SiHa cells was detected by reverse transcription-quantitative PCR. The protein expression of genes in the PI3K/AKT and ITGβ3/TGFβ1 signaling pathways in (C) HeLa and (D) SiHa cells was detected by western blot analysis. Error bars in all panels represent the mean ± SD. *P<0.05, **P<0.01 and ***P<0.001, siCBX7 compared with the control and siCBX7-EVC; $^{\#}$P<0.05, $^{\#\#}$P<0.01 and $^{\#\#\#}$P<0.001, siCBX7 + shRNA TGFβ1 compared with the siCBX7. TGFβ1, transforming growth factor β1; CBX7, chromobox protein homolog 7; PI3K, phosphatidylinositol-3-kinase; ITGβ3, integrin β3; shRNA, short hairpin RNA; CTRL, control; NS, not significant; E-cad, E-cadherin; VIM, vimentin; NC, negative control.

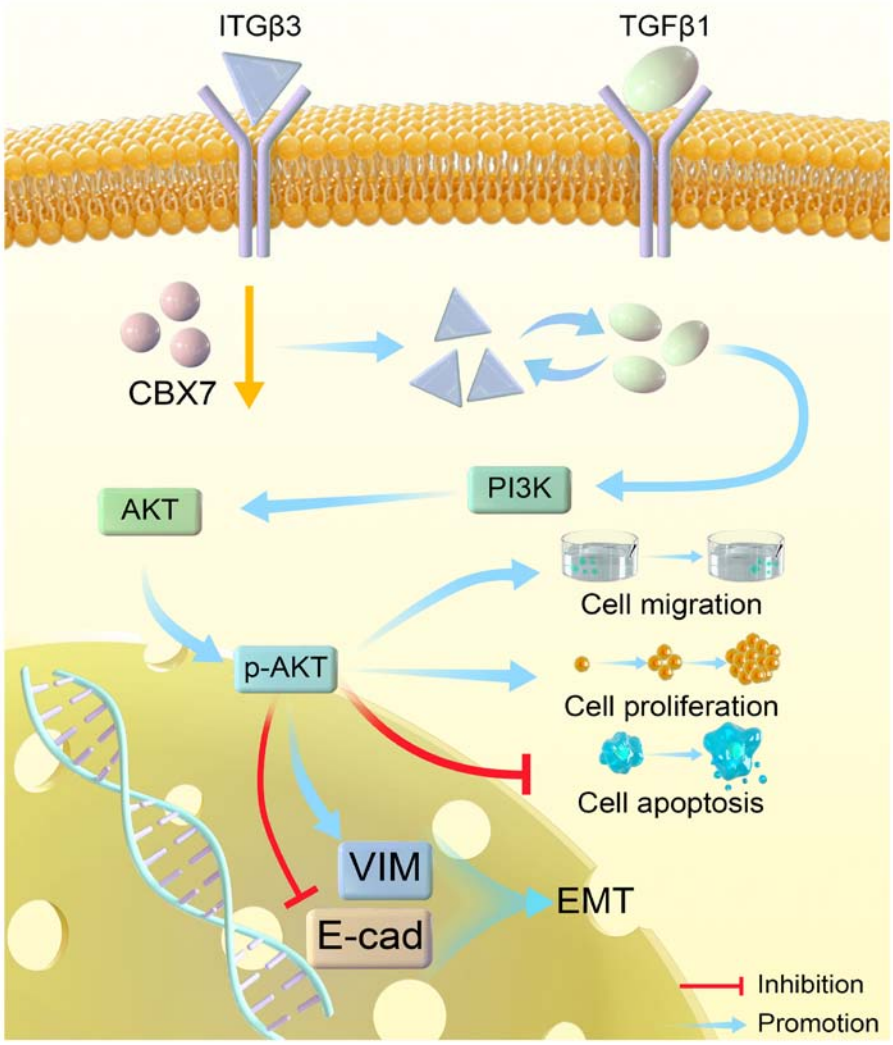

Figure 5. Schematic diagram illustrating the mechanism of CBX7 in cervical cancer. In cervical cancer, downregulation of CBX7 may induce EMT, promote cell proliferation, migration and inhibit cell apoptosis through the ITGβ3/TGFβ1/AKT signaling pathway. CBX7, chromobox protein homolog 7; EMT, epithelial-mesenchymal transition; ITGβ3, integrin β3; TGFβ1, transforming growth factor β1; PI3K, phosphatidylinositol-3-kinase; p-, phosphorylated; VIM, vimentin; E-cad, E-cadherin.

indicated that CBX7 may regulate the proliferation, metastasis and apoptosis of cervical cancer cells through the TGFβ1 signaling pathway. In addition, the expression of key genes of the ITGβ3/TGFβ1 signaling pathway and the EMT process were also analyzed. The RT-qPCR results revealed that the expression levels of *CBX7* and *E-cad* were significantly lower in the siCBX7 group compared with the siCBX7-EVC and CTRL groups, whereas *ITGβ3*, *TGFβ1*, *PI3K*, *AKT* and *VIM* exhibited higher expression levels ($P<0.05$). No differences in CBX7 expression were observed between the cells with silenced and unsilenced TGFβ1. Silencing TGFβ1 in cells resulted in decreased mRNA levels of *ITGβ3*, *PI3K*, *AKT*, and *VIM*, whereas *E-cad* mRNA levels increased (Fig. 4A and B). Western blot analysis demonstrated that silencing TGFβ1 resulted in varying degrees of decrease in ITGβ3, p-PI3K, p-AKT and VIM, except CBX7 and AKT, while E-cad expression increased (Fig. 4C and D). Thus, knockdown of TGFβ1 had no significant effect on CBX7 itself, but partially reversed the activation of the ITGβ3/TGFβ1/AKT signaling pathway and EMT-related genes caused by CBX7 knockdown. These results indicated that knocking down CBX7 may regulate the EMT of cervical cancer cells through the downregulated TGFβ1 signaling pathway.

Discussion

PRC1 is actively expressed in various cancers and participates in tumor progression. As a member of PRC1, CBX7 is a tumor suppressor involved in a variety of cancers (4). Previous studies have revealed that inhibition of CBX7 promotes the migration of gliomas and tumor invasion (10,25). In addition, *in vitro* experiments have confirmed that inhibition of CBX7 promotes the growth of pancreatic cancer (11) and breast cancer (5). CBX7 has also been confirmed to inhibit the growth of liver cancer cells *in vivo* and *in vitro* (26). Recently, in CBX7 knockout mice (9), CBX7 had an inhibitory effect on tumors. CBX7 is involved in tumor growth (12), invasion (6) and migration (27). CBX7 overexpression in urinary bladder cancer cells inhibits tumorigenicity, whereas CBX7 depletion promotes tumor development (28). Moreover, miR-19 affects the migration and cell cycle of lung cancer cells by inhibiting CBX7 expression (29). Consistently, the findings of the

present study revealed that knockdown of CBX7 promoted the migration and invasion of cervical cancer cells *in vitro* and inhibited cell apoptosis. Therefore, low expression of CBX7 may promote tumor progression of cervical cancer.

By analyzing the expression of genes and proteins in human cervical cancer tissues, transplanted tumors in nude mice and cervical cancer cells, downregulation of CBX7 was found to increase the expression of VIM, ITGβ3, TGFβ1, PI3K and AKT, and decrease the expression of E-cad. Furthermore, correlation analysis demonstrated that CBX7 was positively correlated with E-cad and negatively correlated with VIM. Federico *et al* reported that CBX7 positively regulated E-cad expression by interacting with the histone deacetylase 2 protein (30). E-cad and VIM are epithelial and mesenchymal markers of EMT, respectively (31). E-cad can identify cell-cell junctions and apicobasal polarity, limit the migratory potential of epithelial cells and maintain the integrity of tissue structure and function (32,33). The downregulation of E-cad can lead to the destabilization of adherent junctions and promote the transformation of epithelial cells to mesenchymal cells (34). A previous study has shown that the reduction of epithelial phenotype and the increase of mesenchymal phenotype may promote tumor progression (35). Additionally, it has been reported that CBX7 upregulation enhanced E-cad expression (30). In the present study, consistently, it was revealed that knockdown of CBX7 inhibited E-cad and promoted VIM, suggesting that low expression of CBX may promote cervical cancer progression through regulation of EMT. Furthermore, CBX7 can upregulate E-cad (30) and plays a key role in the occurrence of EMT and the progression of advanced cancer (28). Previous research conducted by the authors revealed that CBX7 was downregulated in cervical cancer and its downregulation was associated with a poor prognosis in patients with cervical cancer (22,23). Moreover, it was revealed that CBX7 overexpression inhibited cell proliferation and migration in cervical cancer cells (22,23). Furthermore, the knockdown of CBX7 expression in the present study significantly promoted the migration and invasion of cervical cancer cells. These results strongly suggest that CBX7 may function as a tumor suppressor in the development of cervical cancer. Moreover, it was preliminarily inferred that the low expression of CBX7 involved in the occurrence of cervical cancer EMT may be related to ITGβ3, TGFβ1, PI3K, and AKT signaling pathways, which all play an important role in tumor cell migration and invasion (36,37).

Furthermore, TGFβ1 expression was silenced in cells with stable knockdown of CBX7. TGFβ1 silencing was identified to reduce the migration and invasion of stably transfected HeLa and SiHa cells and increase cell apoptosis. Rapisarda *et al* found that downregulation of CBX7 promoted the expression of ITGβ3 (18). IT5β3/AKT can promote the progression of hemangioendothelioma. Furthermore, research has revealed that TGFβ1 induces the upregulation of integrin alpha V, leading to the promotion of EMT in ovarian cancer cells (38). Intercellular adhesion molecule 1 was demonstrated to promote the migration of triple-negative breast cancer cells through an integrin-mediated mechanism dependent on TGF-β/EMT (39). There is an interaction between TGFβ1 and ITGβ3 (40,41). CBX7 has been revealed to activate PTEN, inhibit the downstream PI3K/AKT pathway, and suppres the proliferation, metastasis and invasion of pancreatic cancer cells (11). In addition, CBX7 was demonstrated to enhance the sensitivity of bladder cancer cells to cisplatin treatment through the inactivation of the PI3K/AKT signaling pathway (42). The TGFβ1 and PI3K/AKT signaling pathways are crucial in regulating diverse cellular responses, such as proliferation, apoptosis and migration (43). PI3K serves as a vital intracellular kinase in organisms, while AKT acts as its most significant downstream factor. The inhibition of TGFβ1 suppresses the occurrence of EMT in cervical cancer cells, thereby restraining cell migration and invasion (44). In the present study, it was found that silencing of TGFβ1 reversed the effects of CBX7 knockdown on the expression of key genes in the ITGβ3/TGFβ1 signaling pathway and the EMT process. Therefore, CBX7 may regulate the progression of cervical cancer through ITGβ3/TGFβ1/AKT signaling pathway (Fig. 5).

The present study has some limitations. Firstly, a subcutaneous xenograft model of cervical cancer cells in nude mice was constructed. However, this model does not accurately replicate the conditions within the nude mice. In the future, the orthotopic transplantation tumor model, which involves transplantation to anatomically relevant sites and exhibits stronger biological relevance to cervical cancer, will be used. Secondly, the present study validated the impact of CBX7 on proliferation, metastasis and apoptosis. However, the factors related to proliferation, metastasis and apoptosis were not examined. The inclusion of these factors in the analysis can enhance the credibility of the conclusions.

In summary, the present study show that low expression of CBX7 is associated with high proliferation and metastasis and low apoptosis of cervical cancer cells. In addition, low expression of CBX7 may affect the PI3K/AKT signaling pathway by upregulating ITGβ3/TGFβ1 and promoting the proliferation of cervical cells and the occurrence of EMT. The findings of the present study provide insights into the mechanisms of cervical cancer and might help the development of potential therapeutic targets for cervical cancer treatment.

Acknowledgements

Not applicable.

Funding

The present study was supported by the State Key Laboratory of Pathogenesis, Prevention and Treatment of High Incidence Diseases in Central Asia Fund (grant nos. SKL-HIDCA-2 020-WF1 and SKL-HIDCA-2022-GJ2), the Postdoctoral Science Foundation of China (grant no. 2019M663963XB), the Xinjiang Autonomous Region Collaborative Innovation Program (grant no. 2019E0282) and the Xinjiang Medical University Student Innovation and Entrepreneurship Training Program (grant no. CX2021046).

Availability of data and materials

The datasets used and/or analyzed during the current study are available from the corresponding author on reasonable request.

Authors' contributions

PT, JD and RL designed the study. PT and JD wrote the manuscript. CM, AM, LD and GM performed experiments. QY, YaL, HM, YuL, CZ and JR collected and analyzed data. All authors have read and approved the final manuscript. PT and RL confirm the authenticity of all raw data.

Ethics approval and consent to participate

The present study was conducted following the Declaration of Helsinki and approved (approval no. 20120220-01) by the Institutional Review Board of Xinjiang Medical University (Urumqi, China). Written informed consent was obtained from all subjects involved in the study. The animal study protocol was approved (approval no. 20120220-01) by the Ethics Committee of Xinjiang Medical University.

Patient consent for publication

Not applicable.

Competing interests

The authors declare that they have no competing interests.

References

1. Sung H, Ferlay J, Siegel RL, Laversanne M, Soerjomataram I, Jemal A and Bray F: Global Cancer Statistics 2020: GLOBOCAN estimates of incidence and mortality worldwide for 36 cancers in 185 countries. CA Cancer J Clin 71: 209-249, 2021.
2. Razzaghi H, Saraiya M, Thompson TD, Henley SJ, Viens L and Wilson R: Five-year relative survival for human papillomavirus-associated cancer sites. Cancer 124: 203-211, 2018.
3. Lee BH: Commentary on: 'Comprehensive molecular characterization of papillary renal-cell carcinoma.' Cancer Genome Atlas Research Network. N Engl J Med. 2016 Jan 14;374(2):135-45. Urol Oncol 35: 578-579, 2017.
4. Forzati F, Federico A, Pallante P, Abbate A, Esposito F, Malapelle U, Sepe R, Palma G, Troncone G, Scarfò M, *et al*: CBX7 is a tumor suppressor in mice and humans. J Clin Invest 122: 612-623, 2012.
5. Iqbal MA, Siddiqui S, Ur Rehman A, Siddiqui FA, Singh P, Kumar B and Saluja D: Multiomics integrative analysis reveals antagonistic roles of CBX2 and CBX7 in metabolic reprogramming of breast cancer. Mol Oncol 15: 1450-1465, 2021.
6. Huang Z, Yan Y, Zhu Z, Liu J, He X, Dalangood S, Li M, Tan M, Cai J, Tang P, *et al*: CBX7 suppresses urinary bladder cancer progression via modulating AKR1B10-ERK signaling. Cell Death Dis 12: 537, 2021.
7. Forzati F, De Martino M, Esposito F, Sepe R, Pellecchia S, Malapelle U, Pellino G, Arra C and Fusco A: miR-155 is positively regulated by CBX7 in mouse embryonic fibroblasts and colon carcinomas, and targets the KRAS oncogene. BMC Cancer 17: 170, 2017.
8. Zheng ZQ, Yuan GQ, Kang NL, Nie QQ, Zhang GG and Wang Z: Chromobox 7/8 serve as independent indicators for glioblastoma via promoting proliferation and invasion of glioma cells. Front Neurol 13: 912039, 2022.
9. Yu T, Wu Y, Hu Q, Zhang J, Nie E, Wu W, Wang X, Wang Y and Liu N: CBX7 is a glioma prognostic marker and induces G1/S arrest via the silencing of CCNE1. Oncotarget 8: 26637-26647, 2017.
10. Li J, Xu Z, Zhou L and Hu K: Expression profile and prognostic values of Chromobox family members in human glioblastoma. Aging (Albany NY) 14: 1910-1931, 2022.
11. Ni S, Wang H, Zhu X, Wan C, Xu J, Lu C, Xiao L, He J, Jiang C, Wang W and He Z: CBX7 suppresses cell proliferation, migration, and invasion through the inhibition of PTEN/Akt signaling in pancreatic cancer. Oncotarget 8: 8010-8021, 2017.
12. Cacciola NA, Sepe R, Forzati F, Federico A, Pellecchia S, Malapelle U, De Stefano A, Rocco D, Fusco A and Pallante P: Restoration of CBX7 expression increases the susceptibility of human lung carcinoma cells to irinotecan treatment. Naunyn Schmiedebergs Arch Pharmacol 388: 1179-1186, 2015.
13. Ni SJ, Zhao LQ, Wang XF, Wu ZH, Hua RX, Wan CH, Zhang JY, Zhang XW, Huang MZ, Gan L, *et al*: CBX7 regulates stem cell-like properties of gastric cancer cells via p16 and AKT-NF-κB-miR-21 pathways. J Hematol Oncol 11: 17, 2018.
14. Scott CL, Gil J, Hernando E, Teruya-Feldstein J, Narita M, Martínez D, Visakorpi T, Mu D, Cordon-Cardo C, Peters G, *et al*: Role of the chromobox protein CBX7 in lymphomagenesis. Proc Natl Acad Sci USA 104: 5389-5394, 2007.
15. Gong L, Tang Y, Jiang L, Tang W and Luo S: Regulation of circ-GOLPH3 and its binding protein CBX7 on the proliferation and apoptosis of prostate cancer cells. Biosci Rep 40: BSR20200936, 2020.
16. Shinjo K, Yamashita Y, Yamamoto E, Akatsuka S, Uno N, Kamiya A, Niimi K, Sakaguchi Y, Nagasaka T, Takahashi T, *et al*: Expression of chromobox homolog 7 (CBX7) is associated with poor prognosis in ovarian clear cell adenocarcinoma via TRAIL-induced apoptotic pathway regulation. Int J Cancer 135: 308-318, 2014.
17. Mosbah A, Barakat R, Nabiel Y and Barakat G: High-risk and low-risk human papilloma virus in association to spontaneous preterm labor: A case-control study in a tertiary center, Egypt. J Matern Fetal Neonatal Med 31: 720-725, 2018.
18. Rapisarda V, Borghesan M, Miguela V, Encheva V, Snijders AP, Lujambio A and O'Loghlen A: Integrin Beta 3 regulates cellular senescence by activating the TGF-β pathway. Cell Rep 18: 2480-2493, 2017.
19. Xiao L, Zhu H, Shu J, Gong D, Zheng D and Gao J: Overexpression of TGF-β1 and SDF-1 in cervical cancer-associated fibroblasts promotes cell growth, invasion and migration. Arch Gynecol Obstet 305: 179-192, 2022.
20. You X, Wang Y, Meng J, Han S, Liu L, Sun Y, Zhang J, Sun S, Li X, Sun W, *et al*: Exosomal miR-663b exposed to TGF-β1 promotes cervical cancer metastasis and epithelial-mesenchymal transition by targeting MGAT3. Oncol Rep 45: 12, 2021.
21. Gu R, Sun X, Chi Y, Zhou Q, Xiang H, Bosco DB, Lai X, Qin C, So KF, Ren Y and Chen XM: Integrin β3/Akt signaling contributes to platelet-induced hemangioendothelioma growth. Sci Rep 7: 6455, 2017.
22. Tian P, Zhang C, Ma C, Ding L, Tao N, Ning L, Wang Y, Yong X, Yan Q, Lin X, *et al*: Decreased chromobox homologue 7 expression is associated with epithelial-mesenchymal transition and poor prognosis in cervical cancer. Open Med (Wars) 16: 410-418, 2021.
23. Li R, Yan Q, Tian P, Wang Y, Wang J, Tao N, Ning L, Lin X, Ding L, Liu J and Ma C: CBX7 inhibits cell growth and motility and induces apoptosis in cervical cancer cells. Mol Ther Oncolytics 15: 108-116, 2019.
24. Larionov A, Krause A and Miller W: A standard curve based method for relative real time PCR data processing. BMC Bioinformatics 6: 62, 2005.
25. Bao Z, Xu X, Liu Y, Chao H, Lin C, Li Z, You Y, Liu N and Ji J: CBX7 negatively regulates migration and invasion in glioma via Wnt/β-catenin pathway inactivation. Oncotarget 8: 39048-39063, 2017.
26. Tan C, Bei C, Zhu X, Zhang Y, Qin L and Tan S: Single nucleotide polymorphisms of CBX4 and CBX7 decrease the risk of hepatocellular carcinoma. Biomed Res Int 2019: 6436825, 2019.
27. Pallante P, Forzati F, Federico A, Arra C and Fusco A: Polycomb protein family member CBX7 plays a critical role in cancer progression. Am J Cancer Res 5: 1594-1601, 2015.
28. Huang Z, Liu J, Yang J, Yan Y, Yang C, He X, Huang R, Tan M, Wu D, Yan J and Shen B: PDE4B induces epithelial-to-mesenchymal transition in bladder cancer cells and is transcriptionally suppressed by CBX7. Front Cell Dev Biol 9: 783050, 2021.
29. Peng X, Guan L and Gao B: miRNA-19 promotes non-small-cell lung cancer cell proliferation via inhibiting CBX7 expression. Onco Targets Ther 11: 8865-8874, 2018.
30. Federico A, Sepe R, Cozzolino F, Piccolo C, Iannone C, Iacobucci I, Pucci P, Monti M and Fusco A: The complex CBX7-PRMT1 has a critical role in regulating E-cadherin gene expression and cell migration. Biochim Biophys Acta Gene Regul Mech 1862: 509-521, 2019.

31. Cicchini C, Amicone L, Alonzi T, Marchetti A, Mancone C and Tripodi M: Molecular mechanisms controlling the phenotype and the EMT/MET dynamics of hepatocyte. Liver Int 35: 302-310, 2015.
32. Wang C, Zhang J, Fok KL, Tsang LL, Ye M, Liu J, Li F, Zhao AZ, Chan HC and Chen H: cd147 induces epithelial-to-mesenchymal transition by disassembling cellular apoptosis susceptibility Protein/E-Cadherin/β-Catenin complex in human endometriosis. Am J Pathol 188: 1597-1607, 2018.
33. Jiang N, Pan W, Li J, Cao T and Shen H: Upregulated Circular RNA hsa_circ_0008433 regulates pathogenesis in endometriosis via miRNA. Reprod Sci 27: 2002-2017, 2020.
34. Vu T and Datta PK: Regulation of EMT in colorectal cancer: A culprit in metastasis. Cancers (Basel) 9: 171, 2017.
35. Loh CY, Chai JY, Tang TF, Wong WF, Sethi G, Shanmugam MK, Chong PP and Looi CY: The E-Cadherin and N-Cadherin switch in epithelial-to-mesenchymal transition: signaling, therapeutic implications, and challenges. Cells 8: 1118, 2019.
36. Luo R, Wei Y, Chen P, Zhang J, Wang L, Wang W, Wang P and Tian W: Mesenchymal stem cells inhibit epithelial-to-mesenchymal transition by modulating the IRE1α branch of the endoplasmic reticulum stress response. Stem Cells Int 2023: 4483776, 2023.
37. E M Eid E, S Alanazi A, Koosha S, A Alrasheedy A, Azam F, M Taban I, Khalilullah H, Sadiq Al-Qubaisi M and A Alshawsh M: Zerumbone induces apoptosis in breast cancer cells by targeting αvβ3 integrin upon Co-administration with TP5-iRGD peptide. Molecules 24: 2554, 2019.
38. Dehghani-Ghobadi Z, Sheikh Hasani S, Arefian E and Hossein G: Wnt5A and TGFβ1 Converges through YAP1 Activity and Integrin Alpha v Up-Regulation promoting epithelial to mesenchymal transition in ovarian cancer cells and mesothelial cell activation. Cells 11: 237, 2022.
39. Chen M, Wu C, Fu Z and Liu S: ICAM1 promotes bone metastasis via integrin-mediated TGF-β/EMT signaling in triple-negative breast cancer. Cancer Sci 113: 3751-3765, 2022.
40. Shidal C, Singh NP, Nagarkatti P and Nagarkatti M: MicroRNA-92 expression in CD133(+) melanoma stem cells regulates immunosuppression in the tumor microenvironment via integrin-dependent activation of TGFβ. Cancer Res 79: 3622-3635, 2019.
41. Fullar A, Dudas J, Olah L, Hollósi P, Papp Z, Sobel G, Karászi K, Paku S, Baghy K and Kovalszky I: Remodeling of extracellular matrix by normal and tumor-associated fibroblasts promotes cervical cancer progression. BMC Cancer 15: 256, 2015.
42. Ren J, Yu H, Li W, Jin X and Yan B: Downregulation of CBX7 induced by EZH2 upregulates FGFR3 expression to reduce sensitivity to cisplatin in bladder cancer. Br J Cancer 128: 232-244, 2023.
43. Chen LY, Cheng CS, Qu C, Wang P, Chen H, Meng ZQ and Chen Z: CBX3 promotes proliferation and regulates glycolysis via suppressing FBP1 in pancreatic cancer. Biochem Biophys Res Commun 500: 691-697, 2018.
44. Huang C, Su T, Xue Y, Cheng C, Lay FD, McKee RA, Li M, Vashisht A, Wohlschlegel J, Novitch BG, *et al*: Cbx3 maintains lineage specificity during neural differentiation. Genes Dev 31: 241-246, 2017.